Electric Power Systems Research 210 (2022) 108135

Contents lists available at ScienceDirect

Electric Power Systems Research

journal homepage: www.elsevier.com/locate/epsr

Comparative evaluation of converter-based compensation schemes for VSC systems to achieve full-range active power transfer in very weak grids

Shuren Wang *, Grain Adam, Khaled H. Ahmed, Barry Williams

Technology and Innovation Centre, University of Strathclyde, Glasgow, UK

ARTICLE INFO

Keywords:
Power converter based grid
Power system
Voltage source converter
Very weak grid

ABSTRACT

Voltage source converter (VSC) is the expected core technology that supports power system de-carbonization by allowing renewable energy development. However, with the increasing penetration of renewables and continuing decommissioning of thermal generators, challenges of integrating VSC-based systems into weak and even very weak ac grids become apparent. Therefore, this paper presents theoretical analysis describing the relationship between active power transfer range and weak grid factors of the generic VSC-grid system, and aims to identify the most effective way to allow the VSC to exchange the rated active power in both directions (±1 pu) with the weak grid. Thus, converter-based compensation is presented to extend the operation boundary and avoid voltage collapsing. Nevertheless, the effects of reactive current provision and series voltage compensations should be recognized; therefore, operational characteristics of two arrangements, namely, shunt and series VSC-based compensation schemes, are comparatively evaluated. In extremely weak grid cases, shunt compensation converter cannot ensure a full active power transfer range of the targeted VSC due to the inherent voltage limitation, whilst series compensation converter can assist the targeted VSC to achieve full-range active power transfer. Effectiveness and performance of the presented compensation methods during power reversal and ac fault are demonstrated with a typical extremely weak grid, and system boundaries with different schemes are given.

1. Introduction

Power electronic interfacing is the norm in modern power systems, including electricity generation, transmission and distribution, and is critical for system operation [1]. Systems with higher penetration of converter-interfaced renewable generation present different characteristics and introduce new technical challenges.

In general, short-circuit ratio (SCR) provides a straightforward quantification of the grid strength at a particular network point and a low SCR indicates low grid voltage controllability due to the high equivalent impedance between the studied point and the equivalent/idealized ac source of the grid [2]. Various variants have been proposed by industrial and academic researchers considering system complicacy, such as weighted SCR (WSCR) [3], composite SCR (CSCR) [4], site-dependent SCR (SDSCR) [5], generalized SCR (gSCR) [6], etc. Nevertheless, equivalent models based on the concepts of SCR and X/R (connection link inductive reactance and resistance ratio) still feature high generalizability for VSC-grid system analysis as in [7–13].

Researchers revealed the voltage source converter (VSC) performance degradation and even instability as the adverse effect of a weak grid (for example SCR < 3) [9]. Various control strategies, with and without phase-locked loops (PLLs), have been proposed to increase converter immunity, stabilize system dynamics, and to decouple control stability from ac grid strength [9–13]. However, although these approaches address the stability issues related to VSC control systems in weak ac grids (usually with the assumption of sufficient reactive current provision), the fundamental problem and solution regarding the active power range curtailment (less than 1 pu) in the extremely weak grid (see, SCR $= 1$) cannot be tackled simply via the control system analysis and design.

As the reactive current provision capability of the VSCs is much lower than that of the thermal generators, ac systems dominated by inverter-based renewable energy sources will exhibit lower grid voltage management capability than thermal generator dominated ones, resulting in decreased ac network strength in general [14,15]. Also, the power rating of converter-based stations is increasing, leading to lower SCRs. The VSC power station is required to operate in either rectifier or inverter mode. For example, VSC-based dc systems can link different ac

* Corresponding author.
E-mail address: shurenwang@ieee.org (S. Wang).

https://doi.org/10.1016/j.epsr.2022.108135
Received 5 December 2021; Received in revised form 27 April 2022; Accepted 23 May 2022
Available online 26 May 2022

networks (as called "interties" or "interconnectors") in order to provide bi-directional power flow support and increase system flexibility [16–18]. Besides, VSC-based dc transmission systems are used in renewable integration applications, whereas the weak grid phenomenon exists especially in the rectifier station that connects renewable sources (such as island/offshore wind farms) via long distance ac transmission links [18,19]. Thus, the transferrable active power may still be reduced due to the insufficiency of reactive current provision and/or converter voltage limitation, which is not desired from the perspectives of grid management and renewable integration. Importantly, a typical VSC is designed for a fixed power capacity, and with pre-defined or possible compromise between active and reactive power outputs [20]. Usually, the voltage rating of an existing VSC station is predetermined by the modulation index, and manipulation of transformer tap changers only converts the device rating issues between voltage and current aspects [21]. Thus, the VSC's normal operation in a weaker grid indicates oversizing the existing converter station, which would be impractical and even impossible [22,23]. In these cases, deploying external compensators would be an inevitable choice in order to retain the normal operation and gain long-term benefits, albeit extra capital expenditures (CapEx) [24]. This retrofitting practice would be even critical for future systems where massive thermal generation is facing decommissioning [25].

To retain the rated power transfer capability without voltage collapse, external grid compensators are suggested. Different approaches have been proposed with respective merits and demerits identified. From a device perspective, mechanical or thyristor-switched capacitor networks are mature and cost-effective amongst reactive power compensation approaches, but flexibility and controllability are inferior [26]. Dynamic reactive power compensation equipment, such as the static synchronous compensator (STATCOM), synchronous condenser, or other FACTS devices, are desirable due to the higher controllability features but usually require higher investment [26–31]. In terms of deployment arrangement, shunt-connected compensation provides reactive power compensation, thereby certain voltage support (regulated at unity) [27,28]. Multiple VSCs with sufficient capacity margin can be parallel-connected to overcome single converter reactive power limitations and introduce more energy sources into the system, which is also a shunt scheme [29]. Series compensation technology is a common practice to compensate long HVAC transmission lines due to its effective line impedance reduction [30, 31]. Research on sub-synchronous and super-synchronous interaction of shunt and series compensators is presented in [32]. However, specific operation features of shunt and series dynamic compensators are not fully investigated for VSC integration applications, especially in terms of power range maximization in very weak grids.

Although VSC's operation in weak grids has been extensively investigated, most publications focused on control system and operational stability perspectives [9–13]. However, it can be observed that the curtailed ac to dc power ranges exist and a full VSC active power transfer range (±1 pu) is not achieved [9–11], indicating that the major research shortfall is that full transferrable active power range (from negative to positive unity) of the VSC in a very weak grid (SCR = 1) has not been investigated. In an effort to address operational challenges regarding the emerging very weak grid scenarios, this paper assesses VSC-based shunt and series compensation arrangements that provide dynamic current/-voltage support, with the priority of enabling the full-range rated active power transfer in such extreme weak grid cases. Clear identification of the factors limiting the active power transfer range of the VSC-grid system is presented. Shunt and series compensation schemes are evaluated to tackle the issue of active power range reduction. The shunt compensator cannot address the active power range curtailment due to an extremely weak grid, while series compensation is a feasible solution to ensure a full-range active power transfer. Technical viability and effectiveness of the analysis are confirmed by simulation, covering both normal and abnormal network conditions.

This paper is organized as follows. Section 2 analyzes generic VSC operating characteristics in a weak ac grid, confirming the necessity of adequate grid compensation to avoid unintended curtailment of active power due to inherent system limits. Then, two VSC-based grid compensation arrangements for weak grids are evaluated in Section 3 in order to maximize the active power transfer range. Section 4 presents simulation results and the conclusion follows in Section 5.

2. Analysis of the VSC in a weak AC grid

2.1. System description

Fig. 1(a) shows a single line diagram of a VSC connected to an ac grid through an interfacing transformer at the point of common coupling (PCC). The equivalent circuit phasor diagram is shown in Fig. 1(b). Phasors $V_C\angle\varphi_C$, $V_P\angle\varphi_P$ and $V_G\angle\varphi_G$ represent converter terminal, PCC and grid internal voltages respectively; $Z_C\angle\theta_C$ and $Z_G\angle\theta_G$ are the interfacing transformer and ac grid impedances respectively; and $I_P\angle\gamma$ is the current that the VSC injects (as the positive direction) at the PCC. The steady-state phasor equations for Fig. 1 are:

$$V_P\angle\phi_P = I_P\angle\gamma Z_G\angle\theta_G + V_G\angle\phi_G \tag{1}$$

$$V_C\angle\phi_C = I_P\angle\gamma Z_C\angle\theta_C + V_P\angle\phi_P \tag{2}$$

$$I_P\angle\gamma = (P_P - jQ_P)/V_P\angle -\phi_P \tag{3}$$

where P_P and Q_P are active and reactive powers at the PCC. Assuming the VSC nominal active power is P_N, the magnitude and phase of ac grid impedance are defined as $Z_G = V_G^2/(A \times P_N)$ and $\theta_G = \tan^{-1}B$, where A and B are SCR and quality factor X/R respectively. For the VSC, $Z_C = \sqrt{X^2+R^2}\ V_G^2/P_N$ and $\theta_C = \tan^{-1}(X/R)$, where X and R are converter transformer inductive and resistive impedances respectively. With substitutions and algebraic manipulation, Eqs. (1) and (2) become:

$$\begin{aligned}&\frac{P_P}{P_N} + B\frac{Q_P}{P_N} + A\sqrt{B^2+1}\cos(\phi_P-\phi_G)\frac{V_P}{V_G} - A\sqrt{B^2+1}\left(\frac{V_P}{V_G}\right)^2\\ &+j\left[B\frac{P_P}{P_N} - \frac{Q_P}{P_N} - A\sqrt{B^2+1}\sin(\phi_P-\phi_G)\frac{V_P}{V_G}\right] = 0\end{aligned} \tag{4}$$

$$\begin{aligned}&R\frac{V_G^2}{V_CV_P}\frac{P_P}{P_N} + X\frac{V_G^2}{V_CV_P}\frac{Q_P}{P_N} + \frac{V_G^2}{V_CV_P} - \cos(\phi_C-\phi_P)\\ &+j\left[X\frac{V_G^2}{V_CV_P}\frac{P_P}{P_N} - R\frac{V_G^2}{V_CV_P}\frac{Q_P}{P_N} - \sin(\phi_C-\phi_P)\right] = 0\end{aligned} \tag{5}$$

After normalization of the system voltage and power variables by their ratings, namely, V_G and P_N respectively (the bar distinguishes per unit from non-per unit), and equating real and imaginary parts of (4) and (5) to zero, the following expressions are obtained:

$$\overline{P}_P + B\overline{Q}_P + A\sqrt{B^2+1}\cos(\phi_P-\phi_G)\overline{V}_P - A\sqrt{B^2+1}\overline{V}_P^2 = 0 \tag{6}$$

$$B\overline{P}_P + \overline{Q}_P - A\sqrt{B^2+1}\sin(\phi_P-\phi_G)\overline{V}_P = 0 \tag{7}$$

$$R\overline{P}_P + X\overline{Q}_P + 1 - \cos(\phi_C-\phi_P)\overline{V}_C\overline{V}_P = 0 \tag{8}$$

$$X\overline{P}_P - R\overline{Q}_P - \sin(\phi_C-\phi_P)\overline{V}_C\overline{V}_P = 0 \tag{9}$$

Eqs. (6) to (9) accurately describe fundamental operation of the VSC-grid system since they do not include approximations nor over-simplifications.

2.2. Operation characteristics

This subsection analyzes generic system operation characteristics with deliberately neglecting of the current and modulation index limits, that is, with unlimited active and reactive power capabilities.

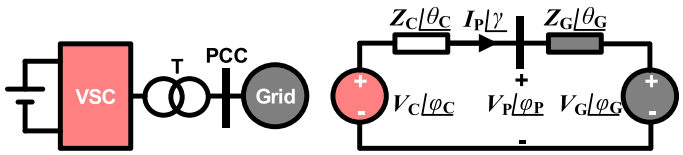

Fig. 1. The generic VSC-grid system. (a) Illustrative diagram. (b) Lumped model with variables.

First, three selected operation point trajectories for different grid X/R values, and with SCR = 1 and V_P = 1 pu, are illustrated in Fig. 2 to demonstrate very weak grid characteristics. The weak grid inductance requires reactive power to achieve active power transfer; whereas the resistance shifts the reactive power and phase angle curves, curtailing active power transfer ranges in such a very weak grid case. This phenomenon jeopardizes the full-range active power transfer feature of the VSC.

The relationship between grid SCR, and PCC active and reactive powers is illustrated in Fig. 3(a). The reactive power and phase-shift angle trajectories for different ac grid strengths, *viz.*, SCR = 1, 2 and 3 (with V_P = 1 pu and X/R = 10) are shown in Fig. 3(b) and (c) respectively. The main observations are:

1) When SCR = 1, the maximum achievable active power exchange range is reduced, particularly, for negative (from the ac to the dc side) active power, in which it is limited to about -0.89 pu. Whilst 1 pu active power exchange remains achievable in the positive (dc to ac) active power range;
2) The required reactive power support at PCC increases drastically with active power exchange between PCC and the ac grid. This rate of increase is exacerbated in the very weak grid (SCR = 1), where, approximately, P_P = -0.89 pu and 1 pu are achieved with Q_P = 0.97 pu and 0.55 pu respectively. Such levels of required capacitive reactive power necessitate excessive use of the VSC, higher dc voltages and increased current capability, or an additional reactive power compensator;
3) The phase-shift angle between V_P and V_G, namely, φ_P - φ_G, increases as the ac grid becomes weaker (SCR decreases), and the maximum power transfer limits for both positive and negative directions are reached before φ_P - φ_G reaches ±90°; and
4) Since the active power limits are reached with φ_P - φ_G < ±90°, it is reasonable to conclude that voltage stability limits are reached primarily; nevertheless, the practically-used VSC interfacing transformer can deteriorate the phase angle issue.

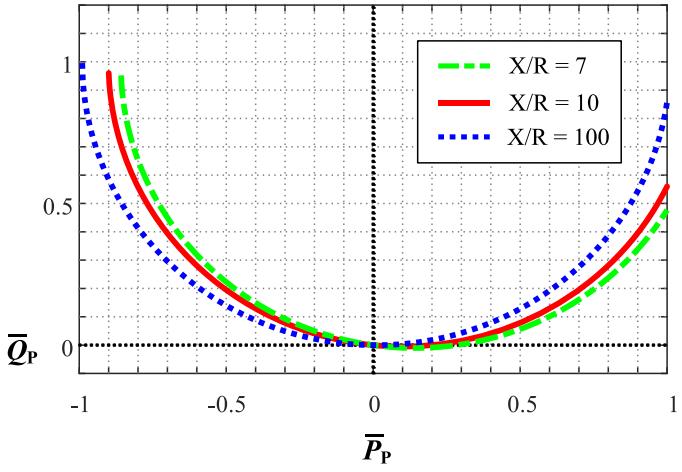

Fig. 2. Relationships between PCC reactive and active power, with three grid X/R values (V_P = 1 pu, SCR = 1).

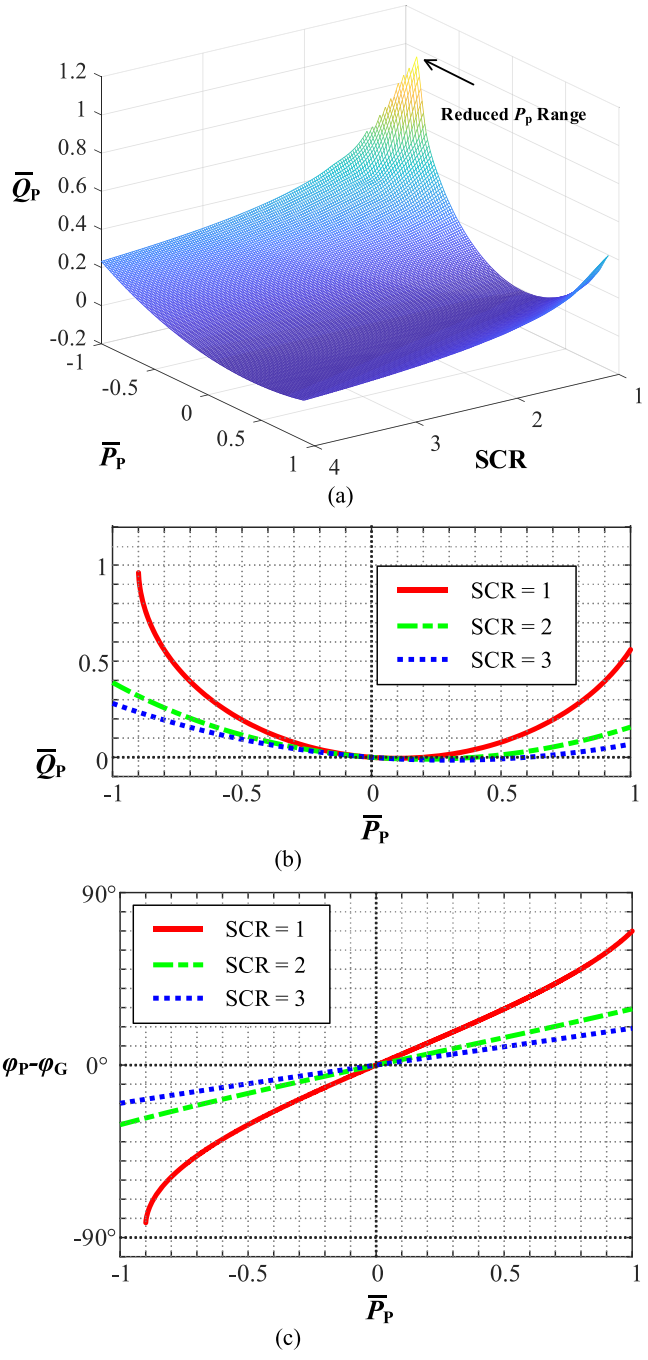

Fig. 3. System characteristics (V_P = 1 pu, X/R = 10). (a) Relationships of SCR, active and reactive power. (b) Reactive and active power with different SCRs. (c) Phase angle and active power with different SCRs.

Importantly, results of further exploratory investigation, in which the ac voltage, and active and reactive power at PCC are varied with the SCR fixed (SCR = 1), are shown in Fig. 4; the main observations are:

1) The increase of PCC voltage V_P extends both voltage and power stability margins, and thereby positive and negative active power transfer ranges;
2) When SCR = 1 and V_P is regulated at higher values than 1 pu, active power exchange between PCC and ac grid can be increased to cover the full range, namely, from the rated positive to the rated negative. But still, these are achieved with significant reactive power support at PCC;
3) When the PCC voltage adheres to a strict regulation (at 1 pu), a full active power transfer range might be impossible, no matter how much reactive power/current is provided; and
4) The existing standards and grid codes that define voltage limits and economic consideration may be questionable for very weak grids.

Therefore, external compensation (in terms of either reactive power or voltage) needs consideration as it has potential to overcome the technical and economic challenges identified from previous discussion and Figs. 2–4.

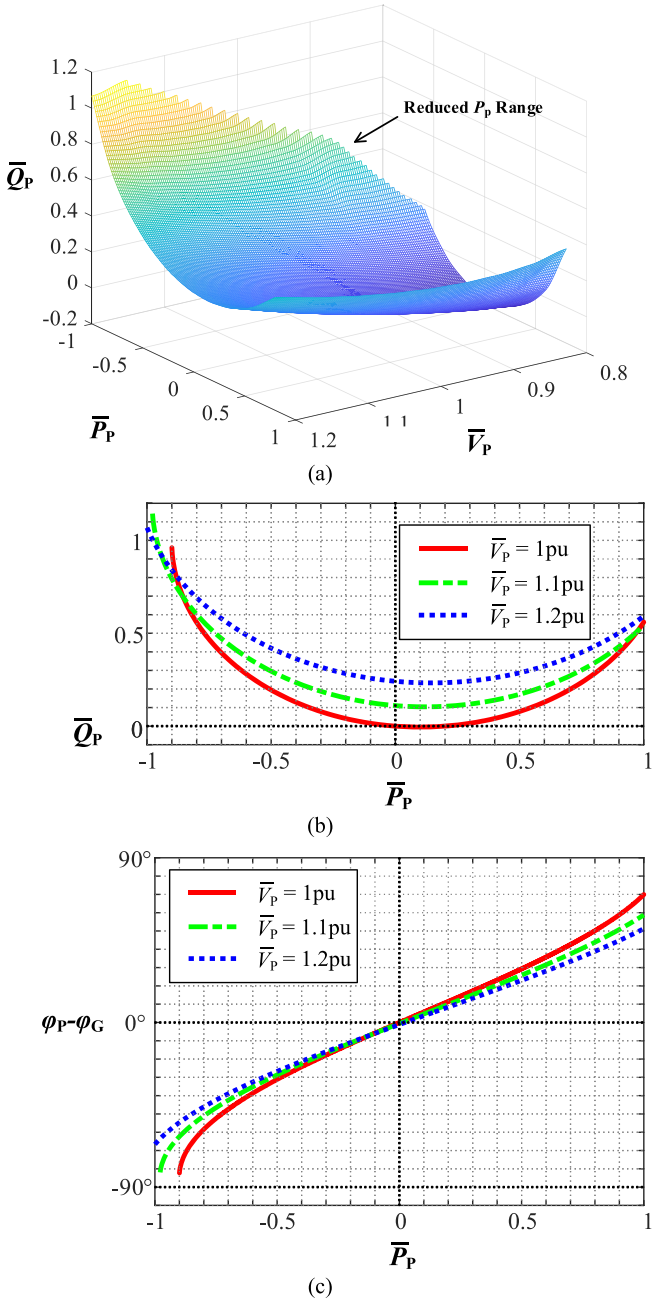

Fig. 4. System characteristics (SCR = 1, X/R = 10). (a) Relationships of voltage, reactive and active power. (b) Reactive and active power with different voltages. (c) Phase angle and active power with different voltages.

3. VSC-based external compensation

Since reactive power support (to maximize active power transfer in a weak ac grid) tends to be significantly larger than the capability of a VSC which is designed primarily for active power application, an external compensating source is generally sought. Therefore, this section discusses and assesses the features and implementation of VSC-based shunt and series grid compensators in a weak ac grid. Fig. 5(a) and (b) show illustrative schemes for shunt and series compensators, in which VSC_I primarily contributes active power P_I and reactive power Q_I; while VSC_{II} and VSC_{III} are shunt and series compensators, contributing reactive power Q_{II} and Q_{III} (active power is controlled to regulate dc-link capacitor voltage).

3.1. Shunt compensation

For the shunt-compensator scheme shown in Fig. 5(a), to ensure ac voltage maintained at 1 pu, the total reactive power provided to the VSC_I PCC (point M) of a weak ac grid is $Q_M = Q_I + Q_{II}$; where Q_I and Q_{II} are the reactive power contributions of VSC_I and VSC_{II} respectively. With PCC voltage $V_M = 1$ pu, active power exchange with the ac grid obeys (6) and (7), and its range is as in Figs 2 and 3. With X denoting interfacing leakage inductive impedance, the reactive power contribution of VSC_{II} is:

$$Q_{II} \approx \left[V_{II}^2 - V_{II}V_M\cos\lambda\right]/X \tag{10}$$

where V_{II} is VSC_{II} terminal ac voltage and λ is the phase-shift angle between V_{II} and V_M. With a 1:1 interfacing transformer ratio, to achieve a positive reactive power contribution ($Q_{II} > 0$), VSC_{II} output voltage should be larger than the PCC voltage ($V_{II} > V_M$).

3.2. Series compensation

A system scheme in which VSC_I is supported by a series compensator

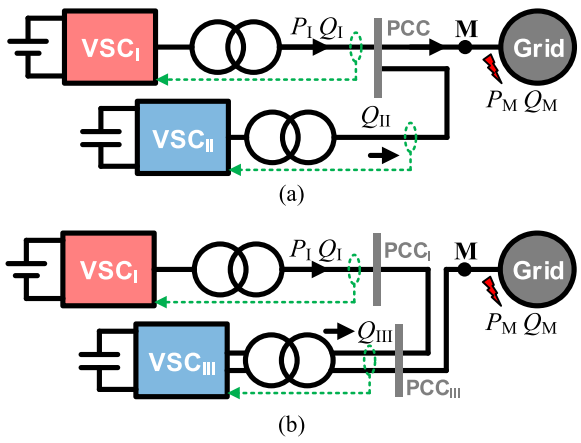

Fig. 5. Power conversion systems with compensators. (a) Shunt compensation with VSC_{II}. (b) Series compensation with VSC_{III}.

VSC_{III} is shown in Fig. 5(b), where the total reactive power provided to point M is $Q_M = Q_I + Q_{III}$. Unlike the shunt counterpart, VSC_{III} reactive power contribution is $Q_{III} = V_{III}I_{ac}\sin\delta$, where V_{III} is VSC_{III} terminal voltage, I_{ac} is ac current flowing through VSC_{III} into the grid, and δ is the phase-shift angle between V_{III} and the ac current. To maintain VSCIII internal capacitor voltage, $|\delta|$ is controlled to be constant at near 90°, in which a small drift is used to compensate for power losses. Thus, reactive power provision of VSC_{III} is approximately:

$$Q_{III} \approx \pm V_{III}I_{ac} - XI_{ac}^2 \tag{11}$$

If the interfacing transformer is not used (which is applicable), to achieve a positive reactive power contribution, the voltage requirement of the series compensator is $|V_{III}| > 0$.

3.3. Comparative discussion

Shunt compensation provides reactive (shunt) current, whereas series compensation is to insert reactive (series) voltage. Fig. 6 illustrates key active power and voltage ranges. Fig. 6(b) shows the achievable negative active power limits of the arrangements without compensation, with a shunt compensator and a series compensator. VSC_I with no external compensation might suffer from the smallest active power range, due to the insufficient converter capacity. This issue can be resolved to some extent by shunt compensation, see Fig. 6(b) where the negative active power limit is extended. However, a full-range negative power transfer with shunt compensation (this includes VSC_I with sufficient inherent capacity) still cannot be achieved due to the voltage limitation. A series compensator can boost the station terminal (point M) voltage and achieve full-range active power transfer, as illustrated in Fig. 6(b). From Fig. 6(c), VSC_I voltage ranges around 1 pu in cases without compensation and with shunt compensation in order to control current and thereby active and reactive powers; whereas output voltage of the VSC_I with a series compensator can be lower than 1 pu (even nullified in extreme cases [19]). Also, the required voltage rating of the series compensator is generally smaller than that of the shunt counterpart, as indicated in Fig. 6(d). Thus, the series compensator capacity to directly neutralize grid impedance impact makes it more effective than the shunt counterpart in terms of voltage utilization (related to the modulation index range), and the generated voltage range can be more flexible. Also, a series compensator enables more effective ac grid voltage support without endangering the main VSC (VSC_I), which might be preferable in very weak grids in future scenarios where more grid flexibility is desired.

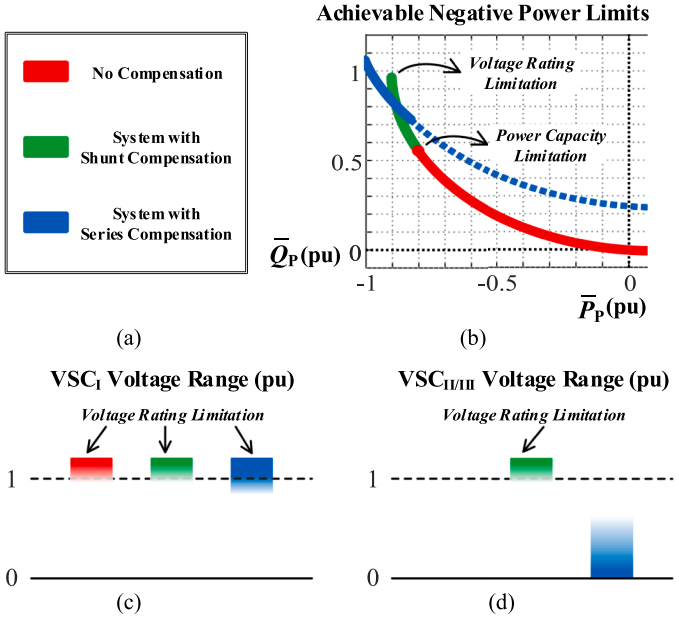

Fig. 6. Illustrative negative power limits and VSC voltage ranges. (a) Legend. (b) Achievable negative power limits of three arrangements. (c) Main VSC_I voltages. (d) Shunt and series compensator voltages.

It was established that with 1 pu PCC voltage, the system active power transfer range might be reduced (from ac to dc) due to the very high ac grid impedance; while a slight PCC voltage rise allows the VSC-grid system to regain its rated active power transfer capability in both directions, thereby retaining system flexibility and controllability. However, a major difficulty is that the converter station equipment, especially the power electronic converters, can be endangered by any potentially increased voltage. In general, a lower voltage rating is desirable for converter design (albeit a higher current rating if active power transfer is required), considering converter manufacturing factors. A large difference between voltage (in hundreds kV) and current (in several kA) magnitudes in high-voltage applications may tip the balance, in terms of cost savings, towards the series compensator. For shunt compensation, simply increasing reactive current injection cannot overcome the voltage magnitude and power transfer limitations, whereas all shunt-connected converters should be oversized (in terms of voltage, current, and/or the interfacing transformer). Nevertheless, the system configuration with series-connected VSCs I and III offers inherent voltage-sharing capability, and could be used to boost the station terminal voltage without jeopardizing critical parts. With the power electronics devices properly protected, the slight overvoltage at station terminal can be easily tolerated with (or even without) minor adjustment of protection measures, which would be similar to the case with series compensation, as reported in [33].

In summary, although a shunt compensation scheme, as a popular practice, can ensure ac grid voltage support (regulated to the rated), potential active power curtailment due to grid weakness cannot be overcome. The series alternative offers an innovative and unique way to handle ac bus voltage flexibly, thereby maximizing the main VSC active power transfer, in very weak grid circumstances.

3.4. Control systems

It has been identified previously that actual system limitation is regarding either voltage or phase angle; therefore control systems are designed to ensure stable operation at the limits with acceptable transient performance, where direct-quadrant (*d-q*) decomposition could be applied with a trade-off between stability and response. Control structures are given in Fig. 7, where VSC_I regulates voltage amplitude at PCC; VSC_{II} and VSC_{III} contribute to weak grid voltage support with reactive power regulation. K_p and K_i in following (15) to (18) are corresponding PI controller gains. The following simulation results show that such grid-following control is still effective for the very weak grid (SCR = 1) applications.

Instantaneous ac current for the VSCs I and II tied to PCC is:

$$v_C = L\frac{di_{ac}}{dt} + Ri_{ac} + v_P \tag{12}$$

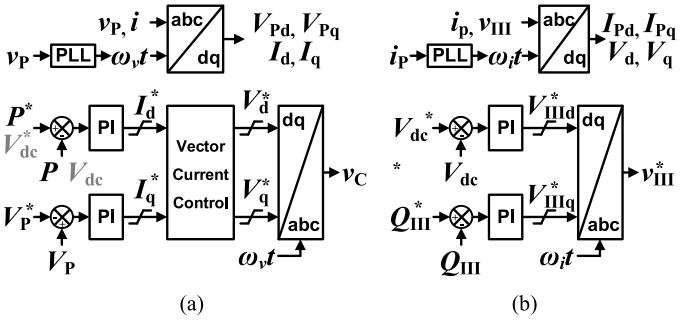

Fig. 7. The adopted control structures. (a) VSC_I and VSC_{II}. (b) VSC_{III}.

where L and R indicate ac impedance between VSC and PCC. Thus, equations describing ac current dynamics are:

$$\frac{dI_d}{dt} = -\frac{R}{L}I_d + \frac{1}{L}\left(V_d - V_{Pd} + \omega L I_q\right) \tag{13}$$

$$\frac{dI_q}{dt} = -\frac{R}{L}I_q + \frac{1}{L}\left(V_q - V_{Pq} - \omega L I_d\right) \tag{14}$$

For VSCs I and II, active power P (or capacitor voltage V_{dc}) and ac voltage V_P (or reactive power Q) control systems are established based on:

$$I_d^* = K_{pM}(M^* - M) + K_{iM}\int (M^* - M)dt \tag{15}$$

$$I_q^* = K_{pN}(N - N^*) + K_{iN}\int (N - N^*)dt \tag{16}$$

where M is P or V_{dc}, N is Q or V_P. As for a current limitation configuration, the q-axis current loop is prioritized to ensure PCC voltage control. For VSC_{III}, since its ac current is controlled by VSC_I, the series voltage to be generated is in line with the ac current as:

$$V_{IIId}^* = K_{pVIIId}({V_{dc}}^* - V_{dc}) + K_{iVIIId}\int ({V_{dc}}^* - V_{dc})dt \tag{17}$$

$$V_{IIIq}^* = K_{pVIIIq}({Q_{III}}^* - Q_{III}) + K_{iVIIIq}\int ({Q_{III}}^* - Q_{III})dt \tag{18}$$

4. Simulation verification

This section focuses on active power transfer capability of the system, considering three arrangements:

1) Case-I: VSC_I with no external compensation,
2) Case-II: VSC_I with shunt compensator VSC_{II}, and
3) Case-III: VSC_I with series compensator VSC_{III}.

Table 1 lists parameters of the MATLAB-Simulink models used to quantitatively evaluate the effectiveness of shunt and series compensators for voltage support or reactive power provision in a very weak ac grid in order to ensure the active power transfer. To compare the normalized values readily, compensators are assumed sized at the system nominal level and compensators II and III are rated the same. Variables are shown in Fig. 5, and positive power flow direction is defined as from the VSC to the ac grid.

Scenarios used to compare and assess performance, particularly, to test the stable and secure operation margin of negative power transfer (from ac to dc side) and ac system fault ride-through during negative power transfer, are:

Table 1
Parameters of the studied systems.

Parts	Items	Values
AC Grid	Nominal Power	200 MW
	Frequency	50 Hz
	Nominal voltage (line-to-line rms)	220 kV
	SCR	1
	X/R	10
VSC_I	DC voltage V_{dc}	200 kV
	Rated power	200 MW
	Transformer ratio	1:1
	Transformer inductance	0.2 pu
	Transformer resistance	0.01 pu
VSC_{II} & VSC_{III}	Rated capacity	200 MVAr
	Capacitive inertia	80 ms
	Transformer ratio	1:1
	Transformer inductance	0.2 pu
	Transformer resistance	0.01 pu

1) Power step change towards the negative extreme, and
2) Asymmetrical grid fault in the negative extreme.

4.1. Step change towards the negative active power extreme

This subsection conducts studies to verify the maximum active power transfer limits of VSC_I by varying its active power set-point in the positive and negative directions until hitting the limits, to verify the theoretical range.

VSCs use a vector current control saturation limit of 1.2 pu (thereby, capable of transferring 1 pu active power while providing 0.66 pu reactive power, ideally). From 0.5 s to 3 s, active power reference of VSC_I is set from -0.8 pu until -1 pu with a step -0.05 pu. For fair comparison, both VSC_{II} and VSC_{III} are controlled to varying its reactive power set-points, to meet reactive power requirements for active power transfer. From 0.5 s to 3 s, the reactive power references of VSC_{II} and VSC_{III} are set from 0.1 pu until 0.5 pu with a step 0.1 pu (0.5 pu is sufficient, if active power is 1 pu, which is in line with the findings from Fig. 4). This configuration is to ensure sufficient reactive power throughout the period without involving more dynamics and VSC interactivity, although compensation of VSCs II and III is adjustable. Also, the modulation index limitation is configured to be 100% rather than smaller in order to test the extreme.

Fig. 8 shows the simulation waveforms of the three cases. Fig. 8I-a to I-d show that, for VSC_I, -0.8 pu active power transfer is achieved with about -0.5 pu reactive current provision, while the PCC voltage magnitude is 1 pu. However, when the active power reference increases at 1 s, VSC_I starts over-modulating, where the modulation index is beyond linear range, see Fig. 8I-a and I-f. At this stage, the 1.2 pu current limit is not reached and I_d and I_q can be barely controlled, see Fig. 8I-b to I-e. After the active power reference becomes -0.9 pu, I_q increases accordingly to regulate PCC voltage (the q-axis is prioritized), while converter current saturation occurs and therefore I_d is limited to near -0.9 pu. Nevertheless, large oscillation can be observed due to the nonlinearity of over-modulation. Thus, Case-I transferable negative active power (from ac to dc side) can be identified between -0.8 pu and -0.85 pu. Waveforms of Case-II in Fig. 8 II-a to II-g show how the shunt compensator VSC_{II} releases the capacity stress upon VSC_I, in a very weak grid. The VSC_I can achieve around -0.9 pu active power transfer (phase angle difference between the VSC_I and the grid source is less than 90°) between 1.5 s and 2 s, with PCC voltage controlled at unity, and with minor over-modulation or current saturation. During this period, VSC_I I_q is around -0.5 pu to support the PCC voltage, and -0.3 pu reactive current needed is provided by the shunt compensator VSC_{II}. After 2 s, both VSC_I modulation index and I_q increase, causing obvious over-modulation and current saturation, but such an operation point shift still cannot allow the rated active power transfer, see Fig. 8 II-b to II-f. VSC_{II} reactive power is tightly controlled throughout this duration, providing sufficient reactive power support for the weak grid, as shown in Fig. 8 II-g. However, VSC_I cannot regulate the PCC properly due to over-range phase angle difference as established in Section 2.2, indicating the voltage control limitation in such a very weak grid case. This result consolidates that the active power transfer is limited to be around -0.9 pu by the PCC voltage limitation issue, no matter how much reactive power is provided (higher extra reactive power with the per unit PCC voltage will only cause saturated converter operation). Comparatively, Fig. 8 Case-III shows system performance with a series compensator. For the main VSC, active power actual value can track its reference to -1 pu, with the PCC voltage at 1 pu, see Fig. 8 III-a and III-b. VSC_I I_d increases to transfer active power whilst I_q increases to regulate VSC_I PCC voltage, without current saturation throughout, as shown in Fig. 8 III-c to III-e. Minor over-modulation occurs due to a voltage drop for the interfacing inductive transformer, and no obvious oscillation is observed, see Fig. 8 III-f. The series compensator VSC_{III} can dynamically provide reactive power into the system, and the voltage of station

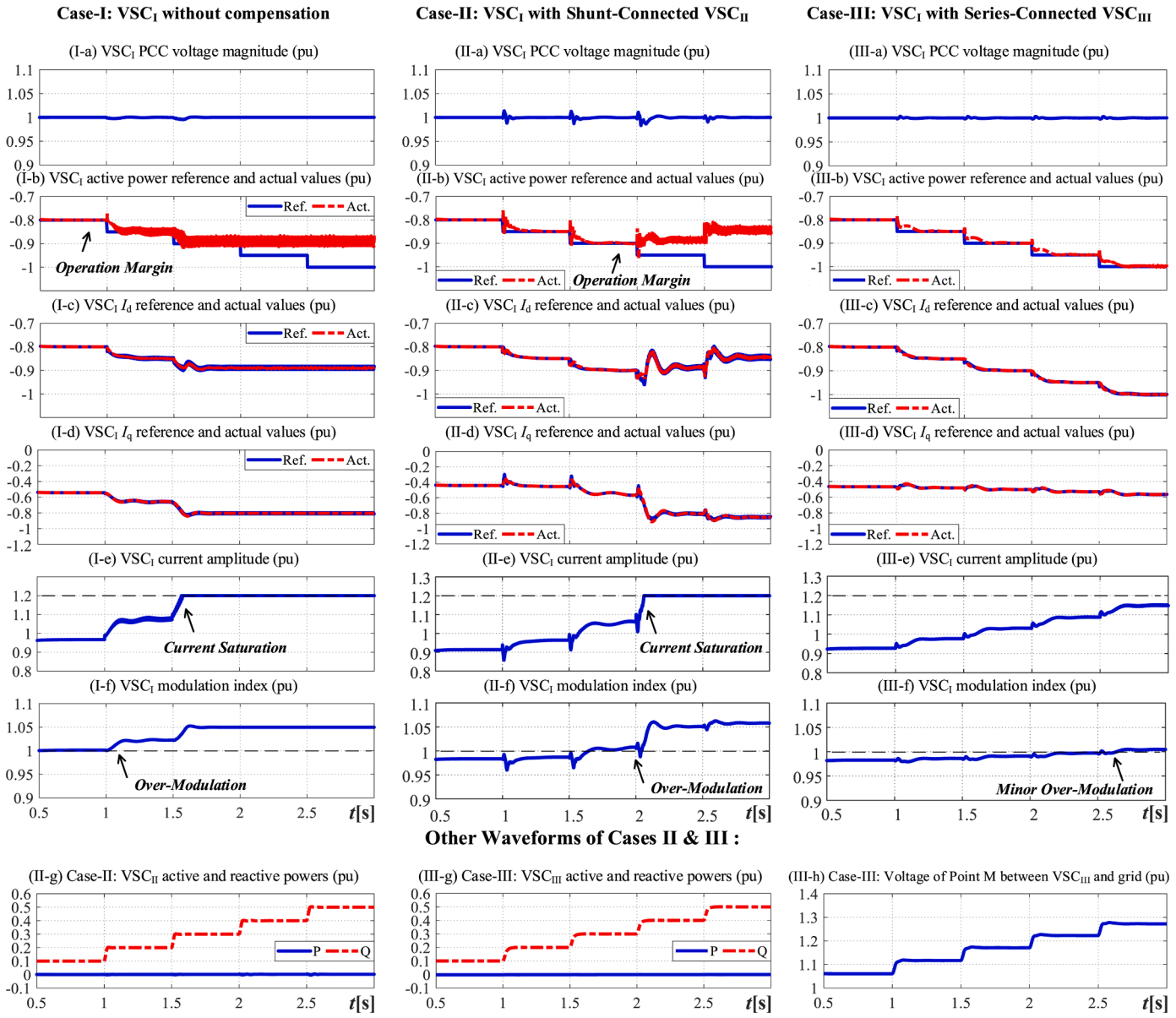

Fig. 8. System step change performance of cases I, II, and III.

terminal (point M between VSC$_{III}$ and the grid) will be effectively increased (to be 1.27 pu in the simulation case), enabling the -1 pu active power transfer, see Fig. 8 III-g and III-h. Thus, the series compensator can ensure VSC$_I$ to achieve full active power transfer range, without causing over-voltage in the main converter station (similar to a static series-capacitor compensator in steady state). These findings are in line with the analysis in Sections 2 and 3.

4.2. Single-phase grid fault

This subsection assesses the fault ride-through performance of the three cases, with a temporary single-phase-to-ground ac fault as shown in Fig. 5. During the pre-fault period, VSC$_I$ transfers -0.82 pu (without compensation), -0.89 pu (with shunt compensation) and -1 pu (with series compensation) active powers, which are close to the negative active power limits that can be drawn from the very weak grid, with the VSC$_I$ rated voltage regulated at 1 pu. During the fault, the ac voltage set points of VSC$_I$ and VSC$_{II}$ are reduced to 0.67 pu in order to avoid excessive over-voltages in healthy phases, with the current limit set to 1.2 pu and with priority to the reactive current provision. VSCs II and III reduce their reactive power contribution to 0.24 pu and 0.3 pu respectively to avoid excessive contribution and converter domination (0.6 times the previous set points).

A solid single-phase-to-ground ac fault occurs at 1 s and is cleared at 1.4 s. The corresponding simulation waveforms are presented in Fig. 9. Fig. 9I-a, II-a and III-a show that the VSC$_I$ PCC voltages are maintained under pre-fault and post-fault conditions and healthy phases do not show significant over-voltage during the fault. AC currents are tightly controlled and limited during the fault, as shown in Fig. 9I-b, II-b and III-b. Fig. 9I-c, II-c and III-c display VSC$_I$ PCC active and reactive powers for the three cases respectively, whereas VSC$_I$ terminal voltages are shown in Fig. 9I-d, II-d and III-d. These results show the system recovers in all cases, which can be attributed to a decrease of active power transfer as the ac voltage at the PCC is actively reduced to 0.67 pu in an effort to increase the voltage stability margin by moving the system operating point away from the point of collapse. Also, no over-voltage occurs at VSC$_I$ terminals in all three cases. Waveforms in Fig. 9 II-e and III-e, and II-f and III-f show reactive power contributions and terminal voltages of the shunt and series compensators (VSCs II and III). VSC$_{II}$ contributes to faulty grid voltage regulation by synthesizing its three-phase voltages to

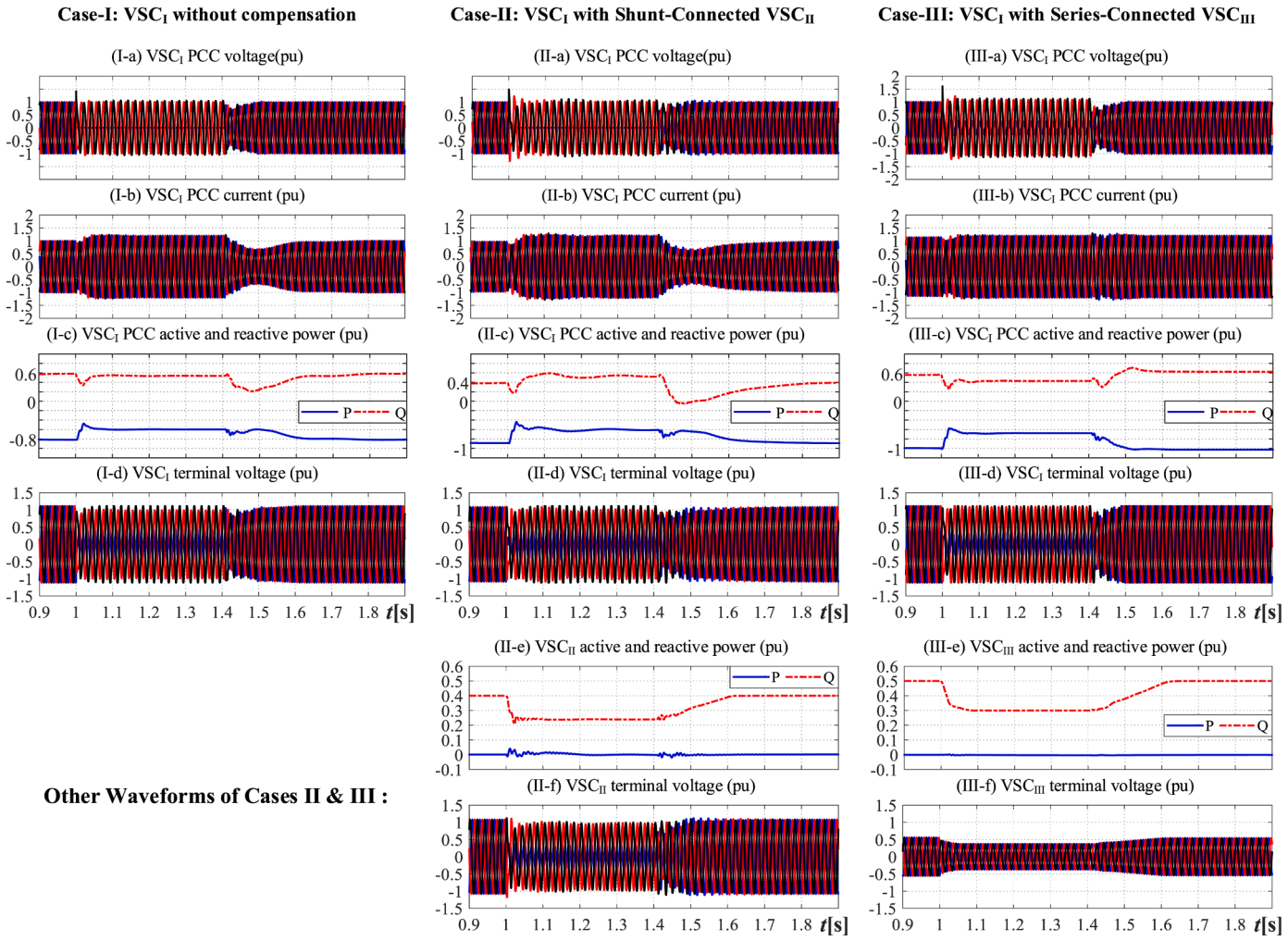

Fig. 9. System grid fault ride-through of cases I, II, and III.

different extents. In contrast, VSC$_{III}$ contributes to reactive power by varying its terminal voltage with the same amplitude as, in this context, VSC$_I$ is responsible for limiting the ac current flowing through the series compensator VSC$_{III}$.

5. Conclusion

This paper presented generic theoretical analysis that describes grid-connected VSC operating trajectory and limits in weak grid scenarios. Considering system operation characteristics, it can be stated that effective reactive power support is the prime condition for the stable operation. Shunt and series VSC-based compensators were comprehensively assessed, whereas the grid-tied VSC with series-connected compensation converter can overcome the active power limitation caused by weak-grid reactance and resistance simultaneously with the flexibly voltage manipulation, facilitating the VSC power transfer maximization. Simulation verification, in a very weak grid scenario (SCR = 1, X/R = 10), was presented to show performance under power reversal and grid fault conditions for cases without and with external compensation. In terms of active power transfer facilitation, the shunt compensator can strengthen the weak ac network for the main VSC, and thereby enlarge the active power range to some extent (by compensating the reactive power rating of the main VSC). The series solution enables the main VSC to transfer active power over the full range and avoids over-voltage of the major devices especially the main VSC. Systems using the converter-based compensation methods can also achieve grid fault ride-through with effective grid voltage regulation. These findings can be used in renewable system construction or grid retrofitting applications.

CRediT authorship contribution statement

Shuren Wang: Conceptualization, Methodology, Investigation, Visualization, Writing – original draft. **Grain Adam:** Conceptualization, Validation, Writing – original draft. **Khaled H. Ahmed:** Visualization, Validation, Supervision, Writing – review & editing. **Barry Williams:** Supervision, Writing – review & editing.

Declaration of Competing Interest

The authors declare that they have no known competing financial interests or personal relationships that could have appeared to influence the work reported in this paper.

References

[1] B. Kroposki, et al., Achieving a 100% renewable grid: operating electric power systems with extremely high levels of variable renewable energy, *IEEE Power Energy Mag.* 15 (2) (Mar. 2017) 61–73, https://doi.org/10.1109/MPE.2016.2637122.
[2] "IEEE guide for planning DC links terminating at AC locations having low short-circuit capacities," 1997, doi: 10.1109/IEEESTD.1997.85949.
[3] Y. Zhang, S.-H.F. Huang, J. Schmall, J. Conto, J. Billo, E. Rehman, Evaluating system strength for large-scale wind plant integration, in: 2014 IEEE PES General Meeting | Conference & Exposition, Jul. 2014, pp. 1–5, https://doi.org/10.1109/PESGM.2014.6939043, vol. 2014-Octob, no. October.

[4] GE Energy Consulting, Minnesota renewable energy integration and transmission study, Schenectady (2014) [Online]. Available, https://mn.gov/commerce-stat/pdfs/mrits-report-2014.pdf.
[5] D. Wu, G. Li, M. Javadi, A.M. Malyscheff, M. Hong, J.N. Jiang, Assessing impact of renewable energy integration on system strength using site-dependent short circuit ratio, IEEE Trans. Sustain. Energy 9 (3) (Jul. 2018) 1072–1080, https://doi.org/10.1109/TSTE.2017.2764871.
[6] L. Huang, H. Xin, Z. Li, P. Ju, H. Yuan, G. Wang, Identification of generalized short-circuit ratio for on-line stability monitoring of wind farms, IEEE Trans. Power Syst. 35 (4) (Jul. 2020) 3282–3285, https://doi.org/10.1109/TPWRS.2020.2975413.
[7] M.F.M. Arani, Y.A.R.I. Mohamed, Analysis and performance enhancement of vector-controlled VSC in HVDC links connected to very weak grids, IEEE Trans. Power Syst. 32 (1) (Jan. 2017) 684–693, https://doi.org/10.1109/TPWRS.2016.2540959.
[8] Ö. Göksu, R. Teodorescu, C.L. Bak, F. Iov, P.C. Kjær, Instability of wind turbine converters during current injection to low voltage grid faults and PLL frequency based stability solution, IEEE Trans. Power Syst. 29 (4) (2014) 1683–1691, https://doi.org/10.1109/TPWRS.2013.2295261.
[9] A. Egea-Alvarez, S. Fekriasl, F. Hassan, O. Gomis-Bellmunt, Advanced vector control for voltage source converters connected to weak grids, IEEE Trans. Power Syst. 30 (6) (2015) 3072–3081, https://doi.org/10.1109/TPWRS.2014.2384596.
[10] Y. Li, et al., Power compensation control for interconnection of weak power systems by VSC-HVDC, IEEE Trans. Power Deliv. 32 (4) (Aug. 2017) 1964–1974, https://doi.org/10.1109/TPWRD.2016.2602890.
[11] S. Lu, Z. Xu, L. Xiao, W. Jiang, X. Bie, Evaluation and enhancement of control strategies for VSC stations under weak grid strengths, IEEE Trans. Power Syst. 33 (2) (2018) 1836–1847, https://doi.org/10.1109/TPWRS.2017.2713703.
[12] Y. Gui, X. Wang, H. Wu, F. Blaabjerg, Voltage-modulated direct power control for a weak grid-connected voltage source inverters, IEEE Trans. Power Electron. 34 (11) (2019) 11383–11395, https://doi.org/10.1109/TPEL.2019.2898268.
[13] G. Wu, et al., Impact of non-minimum-phase zeros on the weak-grid-tied VSC, IEEE Trans. Sustain. Energy (2020) 1–11, https://doi.org/10.1109/TSTE.2020.3034791.
[14] Shun-Hsien Huang, J. Schmall, J. Conto, J. Adams, Yang Zhang, C. Carter, Voltage control challenges on weak grids with high penetration of wind generation: ERCOT experience, in: 2012 IEEE Power and Energy Society General Meeting, Jul. 2012, pp. 1–7, https://doi.org/10.1109/PESGM.2012.6344713.
[15] nationalgridESO, "System operability framework whole system short circuit levels," 2018. [Online]. Available: https://www.nationalgrideso.com/document/135556/download.
[16] K. Sun, H. Xiao, J. Pan, Y. Liu, VSC-HVDC interties for urban power grid enhancement, IEEE Trans. Power Syst. 36 (5) (Sep. 2021) 4745–4753, https://doi.org/10.1109/TPWRS.2021.3067199.
[17] A. Alassi, S. Bañales, O. Ellabban, G. Adam, C. MacIver, HVDC transmission: technology review, market trends and future outlook, Renew. Sustain. Energy Rev. 112 (April) (Sep. 2019) 530–554, https://doi.org/10.1016/j.rser.2019.04.062.
[18] Y. Li, Z. Xu, J. Ostergaard, D.J. Hill, Coordinated control strategies for offshore wind farm integration via VSC-HVDC for system frequency support, IEEE Trans. Energy Convers. 32 (3) (Sep. 2017) 843–856, https://doi.org/10.1109/TEC.2017.2663664.
[19] G.A. Newcombe, "ORION: shaping Shetland as the UK's first green energy island," Sep. 2021, doi: 10.2118/205401-MS.
[20] W. Jiang, Z. Zhang, X. Bie, Z. Xu, Operating area for modular multilevel converter based high-voltage direct current systems, IET Renew. Power Gener. 10 (6) (Jul. 2016) 776–787, https://doi.org/10.1049/iet-rpg.2015.0342.
[21] J.Z. Zhou, A.M. Gole, Rationalisation and validation of dc power transfer limits for voltage sourced converter based high voltage DC transmission, IET Gener. Transm. Distrib. 10 (6) (2016) 1327–1335, https://doi.org/10.1049/iet-gtd.2015.0801.
[22] H. Konishi, A consideration of stable operating power limits in VSC-HVDC systems, in: Seventh International Conference on AC and DC Transmission 2001, 2001, pp. 102–106, https://doi.org/10.1049/cp:20010526.
[23] J.Z. Zhou, A.M. Gole, VSC transmission limitations imposed by AC system strength and AC impedance characteristics, in: IET Conference Publications 2012, 2012, https://doi.org/10.1049/cp.2012.1986.
[24] G. singh Chawda, A.G. Shaik, O.P. Mahela, S. Padmanaban, Performance improvement of weak grid-connected wind energy system using FLSRF controlled DSTATCOM, IEEE Trans. Ind. Electron. 0046 (c) (2022), https://doi.org/10.1109/TIE.2022.3158012, pp. 1–1.
[25] A. Shepherd, S. Roberts, G. Sünnenberg, A. Lovett, A.F.S. Hastings, Scotland's onshore wind energy generation, impact on natural capital & satisfying no-nuclear energy policy, Energy Rep. 7 (Nov. 2021) 7106–7117, https://doi.org/10.1016/j.egyr.2021.10.063.
[26] F.Z. Peng, Flexible AC transmission systems (FACTS) and resilient AC distribution systems (RACDS) in smart grid, Proc. IEEE 105 (11) (2017) 2099–2115, https://doi.org/10.1109/JPROC.2017.2714022.
[27] J.C. Das, Application of STATCOM to an industrial distribution system connected to a weak utility system, IEEE Trans. Ind. Appl. 52 (6) (2016) 5345–5354, https://doi.org/10.1109/TIA.2016.2600657.
[28] M. Nawir, O.D. Adeuyi, G. Wu, J. Liang, Voltage stability analysis and control of wind farms connected to weak grids, in: 13th IET International Conference on AC and DC Power Transmission (ACDC 2017) 2017, 2017, https://doi.org/10.1049/cp.2017.0023, pp. 23 (6 .)-23 (6 .).
[29] F. Alsokhiry, G.P. Adam, Y. Al-Turki, Limitations of voltage source converter in weak ac networks from voltage stability point of view, Int. J. Electr. Power Energy Syst. 119 (January) (Jul. 2020), 105899, https://doi.org/10.1016/j.ijepes.2020.105899.
[30] L. Gyugyi, C.D. Schauder, K.K. Sen, Static synchronous series compensator: a solid-state approach to the series compensation of transmission lines, IEEE Power Eng. Rev. 17 (1) (Jan. 1997), https://doi.org/10.1109/MPER.1997.560708, 62–62.
[31] S. Wang, A.M. Massoud, B.W. Williams, A T-type modular multilevel converter, IEEE J. Emerg. Sel. Top. Power Electron. 9 (1) (Feb. 2021) 843–857, https://doi.org/10.1109/JESTPE.2019.2953007.
[32] D. Shu, X. Xie, H. Rao, X. Gao, Q. Jiang, Y. Huang, Sub- and super-synchronous interactions between STATCOMs and weak AC/DC transmissions with series compensations, IEEE Trans. Power Electron. 33 (9) (Sep. 2018) 7424–7437, https://doi.org/10.1109/TPEL.2017.2769702.
[33] D. Shu, X. Xie, H. Rao, X. Gao, Q. Jiang, Y. Huang, Sub- and super-synchronous interactions between STATCOMs and weak AC/DC transmissions with series compensations, IEEE Trans. Power Electron. 33 (9) (Sep. 2018) 7424–7437, https://doi.org/10.1109/TPEL.2017.2769702.